Electrochemical and Photophysical Properties of Ruthenium(II) Bipyridyl Complexes with Pendant Alkanethiol Chains in Solution and Anchored to Metal Surfaces

Anthony D'Aléo[a], René M. Williams*[,a], Yoël Chriqui[b],Vijay M. Iyer[b], Peter Belser[b], Frank Vergeer[c], Virginia Ruiz[d], Patrick R. Unwin*[,d] and Luisa De Cola*[,a,c]

[a]*Molecular Photonics Group, Van't Hoff Institute for Molecular Sciences, Universiteit van Amsterdam, Nieuwe Achtergracht 129, 1018 WS Amsterdam, The Netherlands*

[b]*Institute of Chemistry, Department of Chemistry, University of Fribourg, Chemin du musée 9, Pérolles 1700 Fribourg, Switzerland*

[c]*Physikalisches Institut, Westfälische Wilhelms-Universität Münster, Mendelstrasse 10, D-48149 Münster, Germany*

[d]*Department of Chemistry, University of Warwick, Gibbet Hill Road, Coventry, CV4 7AL, UK*

Abstract: Luminescent ruthenium trisbipyridine complexes containing one or two mercapto-alkyl chain(s) on one of the bipyridyl units have been synthesized through a new strategy. The electrochemical and photophysical properties, determined in solution and in the solid state were compared. Deposition on electrode surfaces (gold, platinum and indium tin oxide) was realized by self-assembly and the resulting adsorbed layers were characterized by electrochemistry and fluorescence confocal microscopy. Voltammetric measurements of the films, in aqueous and in acetonitrile solution, allowed the determination of the surface coverages and the oxidation potentials of the complexes. The effect of the number of chains and the chain length in the complexes is highlighted. Emission of the adsorbed complexes was strongly quenched by the metallic surfaces, while confocal microscopy images showed aggregate formation on a μm length scale. The latter results provide considerable insight into the nature of the adsorbed layers and support deductions from the voltammetric data.

Keywords: Self assembly, $Ru(bpy)_3$, emission, electrochemistry, transition metal complexes, voltammetry.

1. INTRODUCTION

One of the necessary steps for building up molecular based devices is the crossing over from solution to solid state. Several possible strategies can be followed in order to include "intelligent" components into a matrix, *e.g.* polymerization, blending, evaporation or spin coating. For these methods no precise positioning of the components is attainable. In order to move from disordered solid samples to organized monolayers, it is necessary to assemble the molecules, *via* covalent [1,2,3,4] or non-covalent interactions [5-12] on a substrate and to study their properties at this interface. Amongst the responsive molecules, those addressable with light and able to give a strong emission signal are very appealing since any type of surface can be used and no wiring is required for their activation [13,14].

Consequently, the attachment of photoactive molecules to metal surfaces to develop molecular devices [15-19], nanowire transitor [20,21], sensors [22,23] or photovoltaic systems, able to mimic natural light harvesting and charge separation [24-27] is a very important topic. For these purposes, ruthenium complexes containing polypyridine ligands are very good candidates as they possess light-responsive properties, such as good absorption in the visible region, luminescent and long-lived excited states (triplet Metal-to-Ligand Charge Transfer (^{3}MLCT)) and reversible redox-properties [28,29]. Unfortunately, the functionalization of the coordinated ligands, with *e.g.* mercapto-derivatives, is not straightforward and not many reports have appeared in the literature [30-33].

The attachment of thiol functionalized ruthenium complexes to surfaces such as gold [30,34-36] and platinum [37] as well as semi-conducting surfaces [30] has been reported but there is little information on the quality of the packing, the distance between the chromophore (metal center) and the surface, the orientation of the molecules as well as the coverage, and the stability of the surface when different numbers of anchoring groups are present. Furthermore, a good understanding and correlation between the above mentioned parameters, and the influence of the metal surfaces, on the photophysical properties of complexes is lacking. It is, in fact, predicted that metallic surfaces could quench the emission of attached molecules by energy transfer and/or electron transfer from the luminophore to the surface [38,39]. On the other hand, studies on fluorescent dyes showed that these surfaces can induce an emission enhancement [40-42], as also shown for nanoparticles [43,44]. The latter enhancement phenomenon is used intensively in techniques such as surface enhanced Raman [45-47] or infrared spectroscopy [48-51].

We therefore consider that a complete understanding of the layer formation, quenching processes and electrochemical behavior of luminophores on surfaces is an important

*Address correspondence to these authors at the Molecular Photonics Group, Van 't Hoff Institute for Molecular Science, Faculty of Science, Universiteit van Amsterdam, Nieuwe Achtergracht 129, 1018 WS Amsterdam, Netherlands; Tel: +31 (0)20 525 5477; Fax: +31 (0)20 525 6456; E-mail: williams@science.uva.nl
Physikalisches Institut, Westfälische Wilhelms-Universität Münster, Mendelstrasse 10, D-48149 Münster, Germany;
E-mail: decola@uni-muenster.de
Department of Chemistry, University of Warwick, Gibbet Hill Road, Coventry, CV4 7AL, UK; E-mail: P.R.Unwin@warwick.ac.uk

1874-0987/07

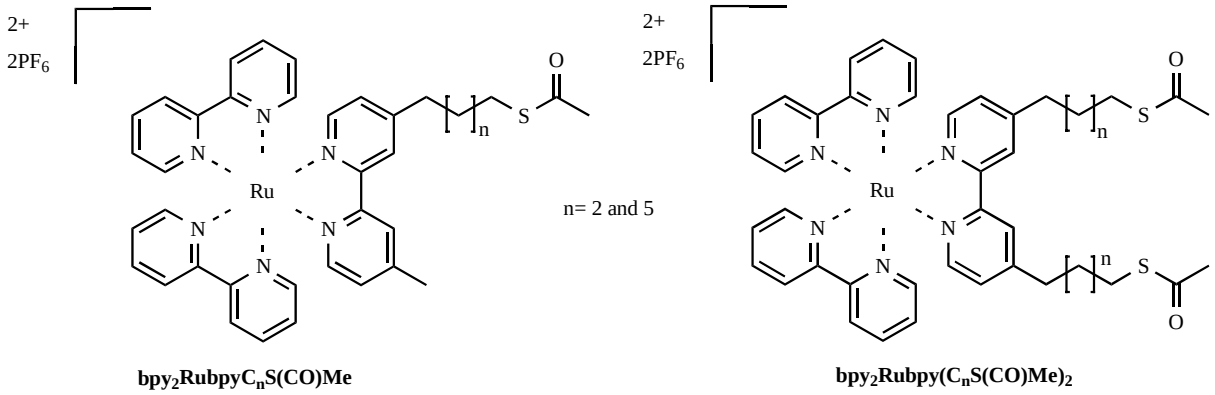

$bpy_2RubpyC_nS(CO)Me$ **$bpy_2Rubpy(C_nS(CO)Me)_2$**

Chart 1. Schematic structures of the thiol protected ruthenium complexes under study.

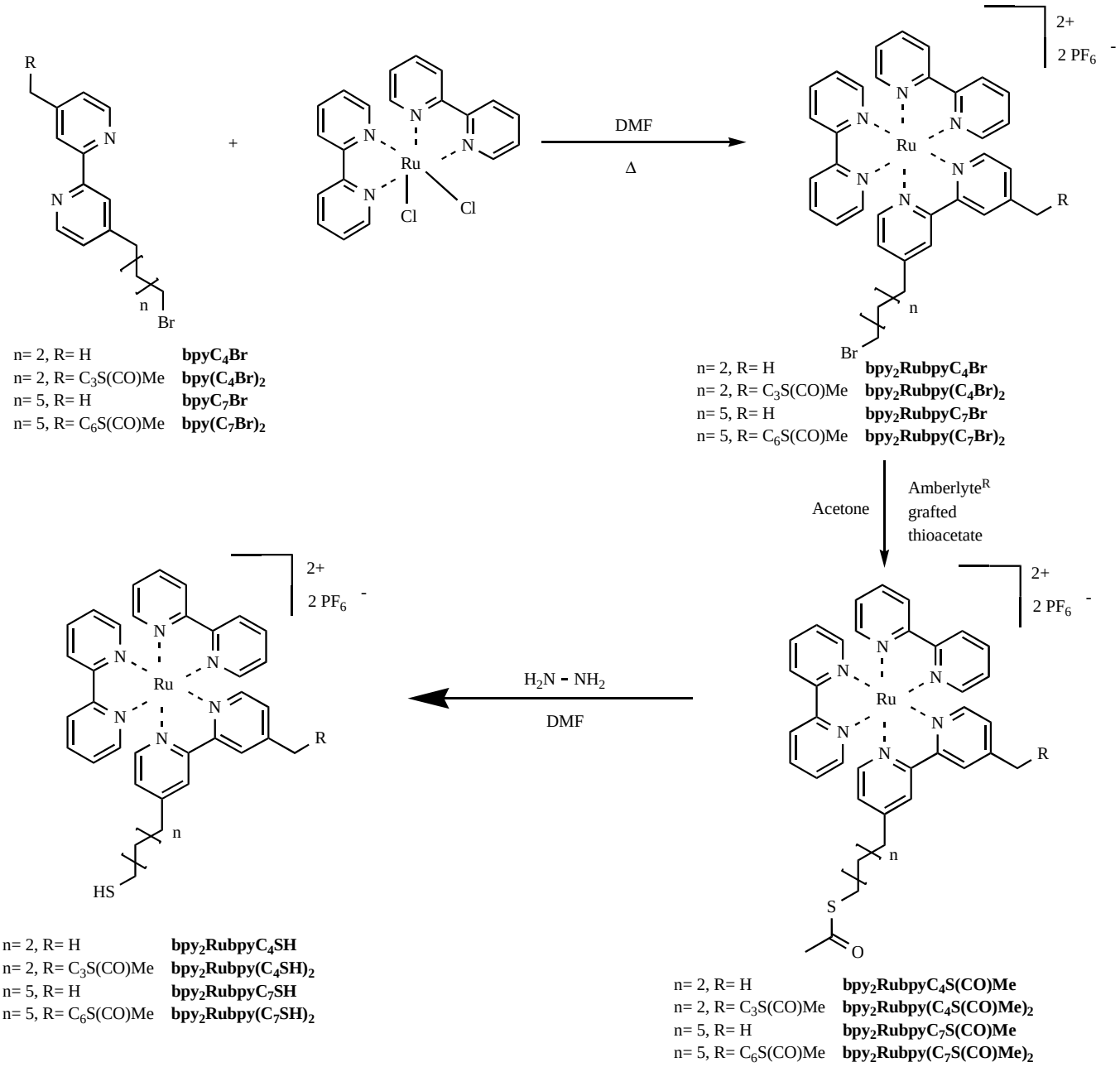

n= 2, R= H	**$bpyC_4Br$**
n= 2, R= $C_3S(CO)Me$	**$bpy(C_4Br)_2$**
n= 5, R= H	**$bpyC_7Br$**
n= 5, R= $C_6S(CO)Me$	**$bpy(C_7Br)_2$**

n= 2, R= H	**$bpy_2RubpyC_4Br$**
n= 2, R= $C_3S(CO)Me$	**$bpy_2Rubpy(C_4Br)_2$**
n= 5, R= H	**$bpy_2RubpyC_7Br$**
n= 5, R= $C_6S(CO)Me$	**$bpy_2Rubpy(C_7Br)_2$**

n= 2, R= H	**$bpy_2RubpyC_4SH$**
n= 2, R= $C_3S(CO)Me$	**$bpy_2Rubpy(C_4SH)_2$**
n= 5, R= H	**$bpy_2RubpyC_7SH$**
n= 5, R= $C_6S(CO)Me$	**$bpy_2Rubpy(C_7SH)_2$**

n= 2, R= H	**$bpy_2RubpyC_4S(CO)Me$**
n= 2, R= $C_3S(CO)Me$	**$bpy_2Rubpy(C_4S(CO)Me)_2$**
n= 5, R= H	**$bpy_2RubpyC_7S(CO)Me$**
n= 5, R= $C_6S(CO)Me$	**$bpy_2Rubpy(C_7S(CO)Me)_2$**

Fig. (1). Synthetic scheme for the preparation of the complexes and the nomenclature used.

step for the development of electroluminescent devices or high-density sensor arrays.

Here we report the synthesis, electrochemistry and photophysical properties of four ruthenium trisbipyridine complexes in which one of the bipyridine ligands has either one or two alkyl chains in the 4,4' position(s) terminated with (protected) thiol group(s) (see Chart **1**). The anchoring of these molecules to different surfaces and the study of the adsorbed layers by electrochemical techniques is described. The differences observed upon variation of the number and the length of these alkanethiol chains is discussed. Furthermore, the photophysical properties of these complexes and the corresponding funcionalized surfaces have been studied using emission spectroscopy and time resolved confocal microscopy.

2. RESULTS AND DISCUSSION

2.1. Synthesis

All the complexes under investigation and their abbreviations are reported in Chart 1. A novel synthetic strategy to prepare thiol derivatives in the 4,4' position of 2,2'-bipyridine (bpy) is described. The bromoalkylbipyridine derivatives were obtained by reacting commercially available 4,4'-dimethyl-2,2'-bipyridine with lithium diisopropylamine . The deprotonated bipyridines were subsequently added to a solution of 1,n-dibromoalkane yielding the mono- or di-alkylated n-bromo-alkylbipyridines.

In order to prepare ruthenium complexes, the bipyridine derivatives were complexed with $[Ru(bpy)_2Cl_2]$ in deaerated DMF. The bromo function(s) were transformed into thioacetate function(s) using an "Amberlyte®" resin grafted with thioacetate (Fig. **1**) [52]. The thioacetate was then deprotected to yield the free thiol by adding hydrazine [53] just before the measurements. All details concerning the synthesis and the characterization are reported in the experimental section.

2.2. Photophysical Properties in Solution

The UV/Visible absorption spectra of these complexes reveal the typical 290 nm band with a molar absorption coefficient around 6 x 10^4 $M^{-1}cm^{-1}$ which is attributed to allowed π-π^* transitions localized on the bipyridyl units [28]. The lower energy absorptions (455 nm) belong to the Metal-to-Ligand Charge Transfer (^{1}MLCT) transitions and are typical for the ruthenium trisbipyridine complexes ($\varepsilon = 1.3 \times 10^4$ $M^{-1}cm^{-1}$). The small red shift compared with the unsubstituted bipyridines is due to the slight electron donating effect of the methyl/alkyl groups attached to the thiolate bpy [54,55]. However, the difference in energy is so small that no separate MLCT bands can be detected. A representative spectrum for the **$bpy_2RubpyC_7S(CO)Me$** complex is shown in Fig. (**2**).

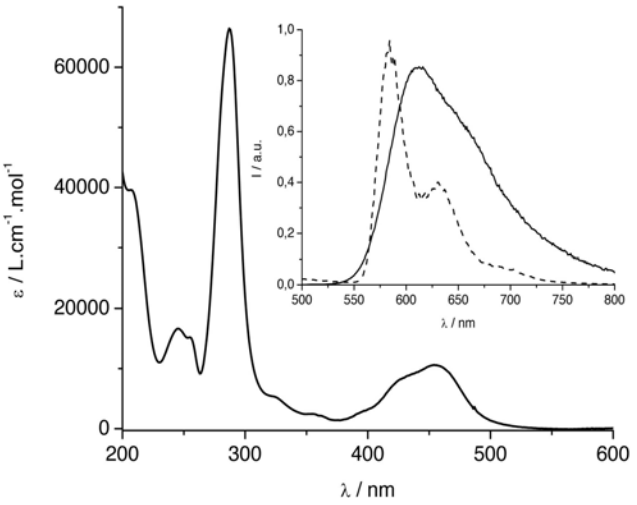

Fig. (2). UV/visible absorption spectrum of **$bpy_2RubpyC_7S(CO)Me$** in acetonitrile. The inset shows emission spectra at room temperature in acetonitrile (dashed line) and at 77K in butyronitrile (solid line).

The emission maxima of these complexes are observed at 616 nm and are attributed to the decay of the ^{3}MLCT state of the ruthenium trisbipyridine complexes. All the complexes have exactly the same emission properties, this is due, as already mentioned, to the slight electron donating properties of the alkyl chain where the lowest excited state involves the unsubstituted bipyridines. The emission lifetimes (150 ns aerated, 1 μs deaerated) of these complexes as well as the quantum yields (0.013 aerated, 0.06 deaerated) are not influenced by the appended alkylthioacetate groups of different lengths. All the data are summarized in Table **1**.

Table 1. Emission Maxima, Emission Quantum Yields and Excited State Lifetimes of the Compounds Under Aerated and Deaerated Conditions at Room Temperature and at 77K

Complex	Luminescence, 298K					Luminescence, 77K	
	λ_{max} (nm)[a]	τ (ns)[a]	τ (ns)[b]	Φ[a]	Φ[b]	λ_{max} (nm)[c]	τ (ns)[c]
$bpy_2RubpyC_4S(CO)Me$	616	149	1069	0.012	0.053	586, 635	2780
$bpy_2Rubpy(C_4S(CO)Me)_2$	615	152	1061	0.012	0.056	586, 635	2766
$bpy_2RubpyC_7S(CO)Me$	615	148	1049	0.013	0.061	586, 635	2888
$bpy_2Rubpy(C_7S(CO)Me)_2$	616	150	1072	0.013	0.060	586, 635	2884

[a] In air equilibrated acetonitrile. [b]In degassed aceonitrile. [c]In butyronitrile glass.

Table 2. Electrochemistry Data in Solution, on Platinum and on ITO

	In solution[a,b]		on Pt[b]			on ITO[c,d]		
Complex	E^0 (V)	ΔEp (mV)†	E^0 (V)	ΔE_P (mV)†	Γ (mol cm^{-2})	E^0 (V)	ΔE_P (mV)†	Γ (mol cm^{-2})
$bpy_2RubpyC_4SH$	0.897	88 ± 3	0.894	37 ± 7	$3.6 \pm 0.6 \cdot 10^{-11}$	1.058	17 ± 3	$5.7 \pm 0.3 \cdot 10^{-12}$
$bpy_2Rubpy(C_4SH)_2$	0.918	53 ± 7	0.900	56 ± 10	$1.8 \pm 0.5 \cdot 10^{-10}$	1.049	8 ± 7	$4.3 \pm 0.5 \cdot 10^{-11}$
$bpy_2RubpyC_7SH$	0.861	63 ± 10	0.895	46 ± 8	$1.2 \pm 0.3 \cdot 10^{-10}$	1.046	8 ± 4	$1.1 \pm 0.2 \cdot 10^{-11}$
$bpy_2Rubpy(C_7SH)_2$	0.906	43 ± 4	0.901	37 ± 9	$1.4 \pm 0.3 \cdot 10^{-10}$	1.064	21 ± 6	$1.3 \pm 0.4 \cdot 10^{-11}$

[a]0.1 M $TBAClO_4$ in acetonitrile. [b]In 0.1 M $TBAClO_4$/acetonitrile; RE was $Ag/AgNO_3$. [c]In 0.5 M H_2SO_4 solution; RE was SCE. [†]up to 1 V s^{-1}. D Coverage was estimated using method described in ref. [30a].

In a solid matrix (77K in butyronitrile glass), the emission maxima are blue shifted, as expected for CT states and already observed for bipyridine complexes (Fig. **1**) [28]. The excited state lifetimes become longer (around 2.8 μs) due to the lack of thermal population of the metal centered, ^{3}MC, state.

2.3. Electrochemical characterization of the complexes in solution and as self-assembled layers

Voltammetric studies were made with the complexes in solution and adsorbed on electrode surfaces. In the latter case, functionalized platinum, gold and indium tin oxide (ITO) surfaces, obtained by a simple immersion technique [56] (see Experimental Section), were investigated using cyclic voltammetry. A summary of peak separation (ΔE_P) and surface coverage (Γ), along with other parameters, is reported in Table **2**.

Attempts to characterize the electrochemical behavior of self-assembled layers of the thiolated complexes on gold surfaces were compromised by the high anodic potential of the $Ru^{II/III}$ redox process for all the complexes, consistent with previous work [31]. However, the presence of a self-assembled layer on gold was evidenced by the substantial decrease of the voltammetric current for water oxidation/reduction (in 0.1 M KNO_3 aqueous solutions) compared to the response of the bare gold surface. Moreover, the presence of adsorbed ruthenium compounds was further evidenced by contact angle measurements with water droplets, which showed an increase in hydrophilicity (contact angles decreased by 14-20°) of the grafted surfaces with respect to the bare gold [57]. This suggested that the hydrophilic ruthenium(II) headgroups in the adsorbed layers were exposed to the water drop. Similar decreases in the contact angle by 12-26° were reported for self assembled layers of **$Ru(bpy)_2(bpy')$** where bpy' = 4-methyl-4'-(dodecyl-1-thiol)-2,2'-bipyridine [30]. The change in hydrophilicity of platinum surface with self assembled layers with respect to bare platinum (contact angle decrease by 14-19°) was comparable to that on gold, tentatively suggesting a similar surface coverage on both metal surfaces.

Successful voltammetry measurements were made on platinum electrodes in acetonitrile solution. Cyclic voltammetry (CV) of the four complexes (0.1 mM complex in acetonitrile/0.1 M Bu_4NClO_4 solutions) was first investigated in solution using a platinum disk as working electrode. Fig. (**3a**) shows a typical CV obtained for the **$bpy_2Rubpy(C_7SH)_2$** complex in solution, demonstrating the high degree of reversibility of the $Ru^{II/III}$ redox process (Nernstian peak separation) even at the highest scan rate examined (10 V s^{-1}). The voltammetric response of the self-adsorbed complex on platinum, recorded in an acetonitrile solution containing only supporting electrolyte (0.1 M $TBAClO_4$), is also shown for comparison (Fig. (**3a**), dashed line). Self assembled adsorbed layers of the four complexes

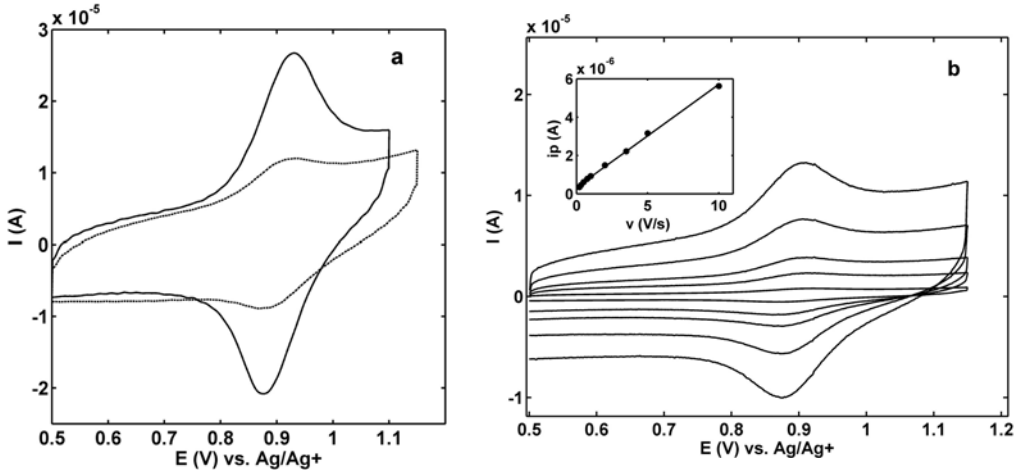

Fig. (3). (a): Cyclic voltammograms of **$bpy_2RuBpy(C_7SH)_2$**: (0.1 mM solution of the complex in acetonitrile/0.1 M Bu_4NClO_4) (solid line) and as SAM on a platinum disk (dashed line). Scan rate 10 V s^{-1}. (b) Cyclic voltammograms of a SAM of **$bpy_2RubpyC_7SH$** on a platinum disk in 0.1 M $TBAClO_4$ in acetonitrile. Scan rates: 0.2, 1, 2, 5 and 10 V s^{-1}. Inset: i_P *vs.* scan rate for the complex as SAM.

on platinum exhibited the characteristic electrochemical behavior of surface-confined species, with very small peak separations at all scan rates (Table **2**) and peak current (i_P) values linearly dependent on scan rate (v) (Fig. (**3b**)).

The high anodic potential of the $Ru^{II/III}$ couple precluded its study on platinum and gold in aqueous solution. However, very well defined voltammograms were obtained for self assembled layers on ITO in 0.5 M H_2SO_4 solutions, as illustrated in Fig. (**4**). The very small separations (8-21 mV) between anodic and cathodic peaks even at the highest scan rates examined (5 Vs^{-1}) were remarkable, showing the high reversibility of the redox process in aqueous media. Moreover, self assembled layers on ITO surfaces proved very stable to repetitive cycling, with the charge remaining constant over one hundred cycles.

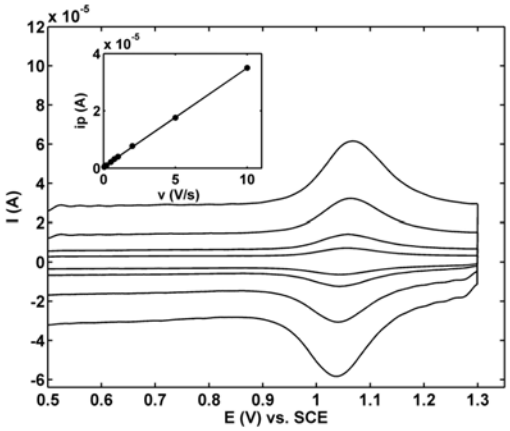

Fig. (4). Cyclic voltammograms of a SAM of **$bpy_2RuBpy(C_4SH)_2$** on ITO ($4.3 \cdot 10^{-11}$ mol cm^{-2}) in 0.5 M H_2SO_4. Scan rates: 1, 2, 5 and 10 Vs^{-1}. Inset: anodic peak current vs. scan rate.

The redox potentials and peak separations of the $Ru^{II/III}$ redox couple are summarized in Table **2** for the four complexes, both in acetonitrile solutions and self-adsorbed on platinum and ITO surfaces. Surface coverage, as estimated by the integration of the anodic wave, is also given in Table **2** for self assembled layers of the four complexes on platinum and ITO. There are no significant differences between the redox potentials of each compound in solution and the value for pre-adsorbed molecules on the electrode surface. Also the redox potentials of the four adsorbed complexes are almost identical. The surface coverage of the four complexes is almost an order of magnitude higher on platinum than on ITO, which agrees well with the expected weaker chemisorption of the thiol groups on ITO surfaces. Although the solvent systems are different, the significantly smaller ΔE_P for the self assembled layers on ITO in aqueous solution, as compared to self assembled layers on platinum in acetonitrile solution, coupled with the much lower surface coverage could suggest a different arrangement of the complexes on the ITO surface. It has been proposed for a similar complex that the molecule could lie flat on an ITO surface [30]. Such an orientation would reduce the distance from the ruthenium centre to the electrode surface with respect to that in self assembled layers on platinum, where the adsorption occurs *via* the sulfur atom. The smaller $Ru^{II/III}$ centre-electrode distance on ITO would explain the faster electron transfer reaction in both directions.

Interestingly surface coverage of three of the complexes on platinum was similar, with the exception of the **$bpy_2RubpyC_4SH$** complex which exhibited a 4-fold lower coverage. At first sight, these results are perhaps surprising since the complexes with two alkyl thiolate chains are expected to possess a better geometry and a stronger chelating effect leading to the formation of more stable adsorbed layers. However, such chelating effect is only observed in the complexes with shorter anchoring chains (comparing the surface coverage of **$bpy_2RubpyC_4SH$** with **$bpy_2Rubpy(C_4SH)_2$)** and not in the two complexes with the longer chains. Also, longer anchoring chains only seem to facilitate higher surface coverage in complexes with only one anchoring group, as evidenced by comparing the surface coverage data of **$bpy_2RubpyC_7SH$** and **$bpy_2RubpyC_4SH$.**

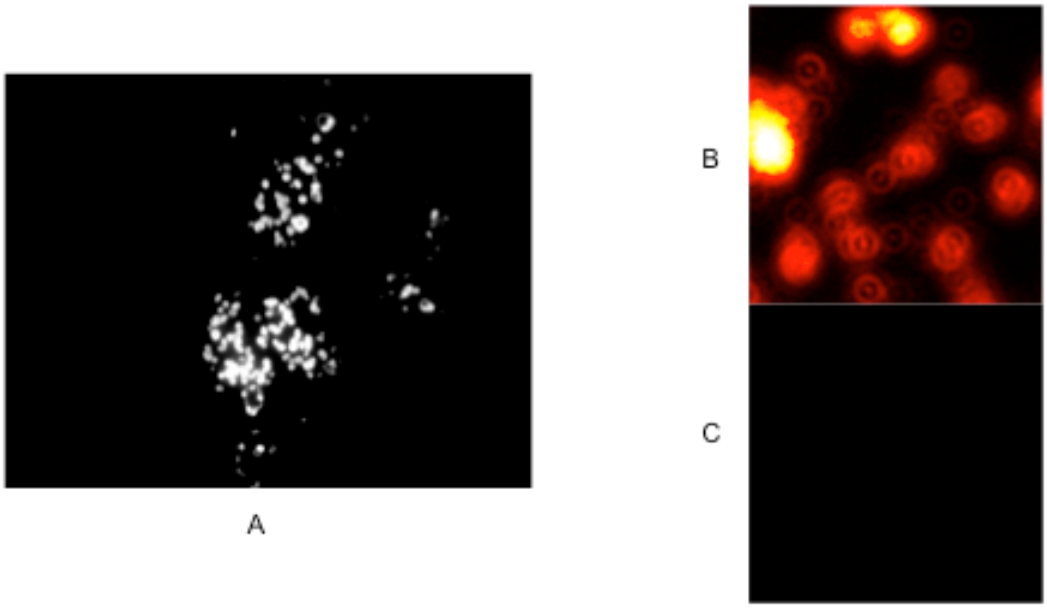

Fig. (5). $bpy_2RuBpyC_7SH$ on A: Fluoresence microscopy of gold surface coated with **$bpy_2RubpyC_7SH$** (85µm by 65µm), B: Confocal microscopic images of SAMs of gold surface coated with **$bpy_2RubpyC_7SH$** (10 µm by 10 µm) obtained in defocus mode, C: Confocal microscopic images of uncoated gold surface (10 µm by 10 µm) using the same highlight threshold as for B.

As on platinum surfaces, **$bpy_2Rubpy(C_4SH)_2$** showed the highest coverage on ITO, 11% (based on an estimated area of 100 $Å^2$/molecule), while for the other complexes, only around 1.5-3% of the surface was covered by the adsorbate. These results, combined with the surface coverage on platinum, showed that the optimum number of carbon atoms spacing the ruthenium centre from the sulfur atom or the optimum number of tails are parameters which are difficult to tune. From these results, it can be concluded that, in complexes with short tails, two anchoring groups result in more efficient coverage whereas with longer chains complexes with two chains appear to lead to similar coverages as those with single chains of the same length.

2.4. Photophysics of the functionalized surfaces

The photophysical behavior of the complexes **$bpy_2RubpyC_4SH$**, **$bpy_2Rubpy(C_4SH)_2$**, **$bpy_2RubpyC_7SH$**, and **$bpy_2Rubpy(C_7SH)_2$** on the different surfaces were investigated using emission spectroscopy. Attempts to record emission spectra with a conventional spectrofluorimeter were unsuccessful because of the weakness of the signals and the high scattering of the metal substrates. Therefore, the solid samples were investigated by fluorescence and confocal microscopy.

Fluorescence microscopy investigations showed that the complexes are not uniformly distributed on the entire surface but they tend to aggregate in smaller islands (Fig. **5A**). To understand the effect of the surface on the photophysical behavior confocal microscopy experiments were performed on gold and platinum substrates.

Selective observation of the ruthenium emission (λ_{ex}= 440 nm; λ_{det}= 580-680 nm) resulted in dotted patterns with an irregular distribution. These dots appeared as concentric rings (Fig. **5**) when using the defocus mode (diffraction of the emission of the substrate) [58,59]. The in-homogeneity of the surface coverage was confirmed by the intensity of the emitted light that was not equal over the observed area. Furthermore, when increasing the highlight value, some spots disappeared. Given that the spot sizes are at the diffraction limit, the different emission intensities are most likely due to domains on the surface, which have different lateral dimensions, but are all smaller than the diffraction limit (Fig. **6**). Most significantly, these patterns indicate that distinct island formation occurs, rather than a homogeneous layer. It is apparent that, on the visualization of adsorbate irregularities, these results are consistent with the low coverage (between 9 and 47 %) observed for all metal surfaces (see electrochemical characterization).

Table 3. Lifetimes Found on Gold and Platinum Surfaces (τ_{av} is the Averaged Lifetimes Observed Determined on at Least 3 Different Spots)

	Lifetimes (τ / ns)	
	τ_{av} (platinum)	τ_{av} (gold)
$bpy_2RubpyC_4SH$	3	7
$bpy_2Rubpy(C_4SH)_2$	4	8
$bpy_2RubpyC_7SH$	3.5	6
$bpy_2Rubpy(C_7SH)_2$	4	7

On platinum and gold surfaces, the emission lifetimes of ruthenium complexes were determined (Table **3**). On platinum, analysis of the decay curves resulted in a biexponential fit, consisting of a long-lived component (around 3-4 ns for all species) and a pulse-delimited component (200 ps). The latter component was then attributed to the laser light reflected by the metallic surfaces because of identical results when the measurements were performed on a bare platinum surface. The 3-4 ns component (τ) can be attributed to the ruthenium complexes present on the surface indicating that quenching occurs in such an assembly. Furthermore, similar measurements on a gold surface also revealed two components, with one arising from the bare surface and the second attributable to the attached ruthenium center. On this surface, lifetimes of around 6 ns were found, which are substantially longer than observed on platinum. To prove that the complexes were covalently linked to the surfaces *via* the thiol functionality, several attempts were made to adsorb $Ru(bpy)_3^{2+}$ on the metallic surfaces but no coverage was detected. Therefore, to obtain a lifetime reference value (τ_0), the emissive lifetime of ruthenium trisbipyridine powder on glass was detected (180 ns). Based on the difference in lifetime, between the complexes on gold and glass, we can conclude that energy/electron transfer from the ruthenium center to the gold surface does occur, with a relatively slow rate constant. The rate k_{eT} can be calculated from [60]:

$$k_{eT} = 1/\tau - 1/\tau_0$$

yielding a transfer rate constant of 2.8×10^8 s^{-1} on platinum and 1.7×10^8 s^{-1} on gold. This rate constant has to be seen in the light of the structure of the complexes on the surfaces, which is dominated by island formation.

In view of these results, we conclude that we observe an average energy transfer rate that is the combination of the rates in layers of different dimensions but still, the quenching noticed is high for both surfaces in comparison to ruthenium trisbipyridine powder deposited on a surface.

3. CONCLUSIONS

The electrochemical and photophysical properties of ruthenium (II) trisbipyridine complexes with pendant alkanethiol chains were determined in solution and anchored to metal surfaces. In solution, the photophysical and electrochemical behaviour of the substituted ruthenium complexes are similar to those of $Ru(bpy)_3^{2+}$.

Contact angle measurements on the self assembled layers show that a hydrophilic surface is formed and electrochemistry indicates a surface coverage between 2 and 47 %, depending on the number of chains, their length and the type of surface. Confocal microscopy shows island formation and time resolved emission indicates an averaged life time of 4 ns on platinum and 6 ns on gold from which energy/electron transfer quenching rate constants were obtained (2.8×10^8 s^{-1} and 1.7×10^8 s^{-1}, respectively).

It is clear that the lack of a good organization on the surfaces is an important issue for the use of such complexes in nano-devices. The assembly led to the quenching of the emission, however a strong correlation between the distance, the anchoring points and the emission lifetime was not observed. The shape, and perhaps the charge, of the complexes are likely to play an important role in the assembly process

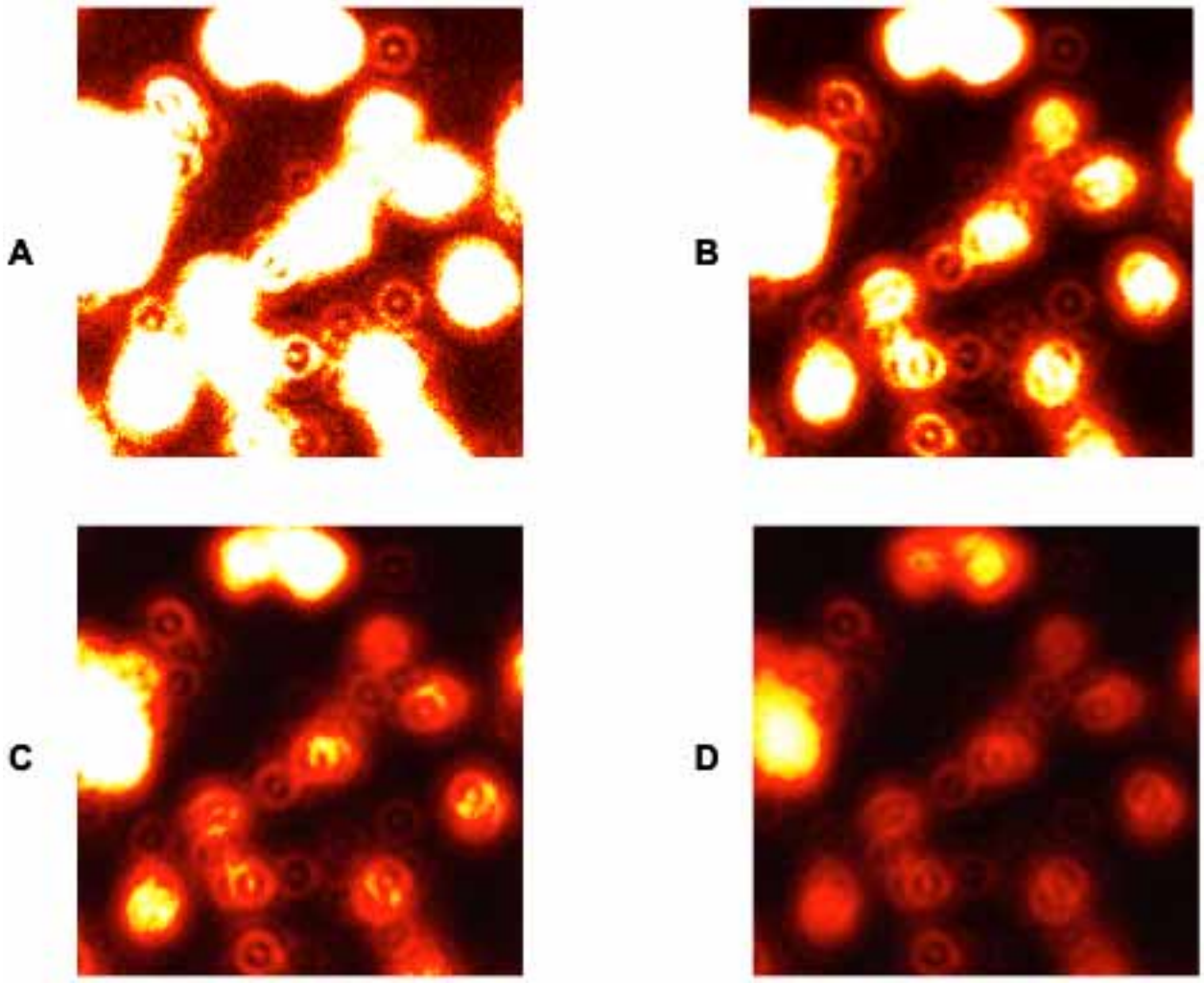

Fig. (6). Confocal microscopic images of **$bpy_2RubpyC_7SH$** on gold surface with increasing the highlight (10 μm by 10 μm), obtained in defocus mode.

and an improved methodology must be envisaged to obtain a high surface coverage and a better quality of the adsorbed layer with this type of complexes.

ACKNOWLEDGEMENTS

We wish to thank the EU projects SUSANA (HPRN-CT-2002-00185) and MWFM (G5RD-CT-2002-00776) and the Alexander von Humbold Foundation for financial support.

4. EXPERIMENTAL PART

General

All chemicals were purchased from Acros or Aldrich and were used as received. All solvents for synthesis were of analytical grade and used without further purification. For the spectroscopy, spectroscopic grade solvents were used. ^{1}H-NMR spectra were recorded on a Varian Gemini-300 spectrometer. Chemical shifts (δ) are given in ppm, using the deuterated solvent as internal standard.

Photophysical Measurements

The UV/vis absorption spectra were recorded on a Hewlett Packard diode array 8453 spectrophotometer. Recording of the emission spectra was done with a SPEX 1681 Fluorolog spectrofluorometer. Low temperature emission spectra for glasses and solid state samples were recorded in 5 mm diameter quartz tubes that were placed in a Dewar filled with liquid nitrogen and equipped with quartz walls. The emission spectra were corrected for monochromator and photomultiplier efficiency and for xenon lamp instability. Lifetimes were determined using a Coherent Infinity Nd:YAG-XPO laser (1 ns pulses FWHM) and a Hamamatsu C5680-21 streak camera equipped with a Hamamatsu M5677 low speed single sweep unit.

A sub-nanosecond single photon counting setup was used for time-resolved fluorescence measurements. The excitation source consisted of a frequency doubled (300 – 340 nm, 1 ps, 3.8 MHz) output of a cavity dumped DCM dye laser (Coherent model 700) that was pumped by a mode-locked Ar-ion laser (Coherent 486 AS Mode Locker, Coherent Innova 200 laser). A microchannel plate photomultiplier (Hamamatsu R3809) was used as the detector.

Cleaning of Substrates and Preparation of Self Assembled Layers

Prior to use, ITO films on glass (Delta Technologies, Ltd., USA) were cleaned by sequential sonication (10 min) in water, absolute ethanol and propanol, and rinsed again

with water just before use. Gold and platinum films (100 nm thick) were evaporated on glass using a 10 nm thick adhesive underlayer of chromium or titanium respectively. The films were cleaned in Piranha solution for 20 min, rinsed with water and ethanol and dried with N_2 (CAUTION: Piranha solution can react violently with organic material and should be handled with extreme caution). Platinum disks were cleaned mechanically by polishing with 0.05 μm alumina (Buehler) on a polishing cloth (Buehler), rinsing with water and sonicating in water for 10 min. The electrodes were then placed in a hot concentrated nitric acid solution for 10 min. Finally, the electrodes were cycled between +1.8 and –0.8 V at 4 $V \cdot s^{-1}$ for 2 min in a 1 M sulfuric acid solution.

For voltammetric measurements on self assembled layers, the ruthenium complexes were allowed to adsorb onto the electrode surfaces by immersing the clean substrates in 1 mM solutions of the ruthenium complexes in acetonitrile overnight. Next, the substrates were rinsed with acetonitrile and methanol to remove any physisorbed material after which they were finally dried with N_2.

Electrochemical Measurements

Cyclic voltammetry (CV) measurements were made in a three-electrode arrangement using an electrochemical analyser (CH Instruments, model CHI 400). A platinum wire was always used as the counter electrode. Different working electrodes were employed, such as ITO (0.14 cm^2), a platinum disk (1.6 mm diameter, area 0.02 cm^2) and both platinum and gold thin films deposited on glass (100 nm thick, area 0.25 cm^2). A saturated calomel electrode (SCE) was used as the reference electrode in aqueous solutions and an $Ag/AgNO_3$ reference electrode (157 mV vs. SCE) was employed in 0.1 M Bu_4N ClO_4/acetonitrile solutions.

Contact Angle Measurements

Dynamic contact angle measurements were made with Milli-Q water under ambient conditions. Water drops (5 μL) were placed at five different spots on the substrate surface and the average of these measurements is reported.

Confocal Microscopy Measurements

Confocal microscopy images were obtained with a MicroTime 200 fluorescence lifetime microscope system (Picoquant) coupled to an Olympus IX71 inverted microscope. The excitation source consisted of a pulsed blue-diode laser (PDL 800-B, PicoQuant Berlin) with a wavelength of 440 nm, providing output pulses of < 100 ps. All measurements were conducted in a dark compartment at room temperature in air.

Fluorescence Microscopy

An epi-fluorescence microscope (Axioplan, Germany), equipped with a 63x long distance objective (NA 0.90) and standard fluorescence filter sets, was used. Images were taken by a CCD camera (KAPPA, Germany), digitized by a frame-grabber card, and processed by imaging software.

4-(4-Bromo-1-butyl)-4'-(methyl)-2,2'-bipyridine (bpyC$_4$Br)

In a 100 mL Schlenk flask, distilled diisopropylamine (1.14 mL, 8.14 mmol) was added to dry THF (20 mL) under nitrogen. The solution was cooled to -68 °C and *n*-butyllithium (6.51 mmol) was added dropwise. The resulting lithiumdiisopropylamine (LDA) solution was stirred at this temperature during one hour and was then allowed to reach room temperature.

In a 250 mL flask, 4,4'-dimethyl-2,2'-bipyridine (1.00 g, 5.43 mmol) was solubilized in dry THF (100 mL). The solution was cooled to -68°C. Then, the above-prepared solution of LDA was added dropwise over a period of 30 min after which the solution was stirred for another 45 min. After this period the solution was allowed to reach room temperature.

In a 500 mL flask (high dilution conditions), the above-prepared bipyridine solution was slowly added to a cooled solution (-68°C) of 1,6-dibromopropane (21.9 g, 108 mmol) in dry THF. The resulting solution was stirred for one hour and then allowed to reach room temperature. Finally, the solution was stirred at room temperature for 14 hours.

The reaction was quenched with HBr 48% (5 mL) and the solution was concentrated under vacuum. The precipitate was filtered off and dissolved in water. Then, K_2CO_3 was added until pH = 7 was reached. Finally, the aqueous layer was then extracted with chloroform, dried with $MgSO_4$ filtered and the solvent was evaporated under vacuum.

Yield: 21% (M = 305.22 g mol^{-1}, $C_{15}H_{17}N_2Br$), ^{1}H-NMR (300 MHz; CD_2Cl_2): ∂ (ppm) = 8.55 (m, 2H), 8.25 (s, 2H), 7.14 (d, ^3J = 7.1 Hz, 2H), 3.40 (t, ^3J = 6.9 Hz, 2H), 2.70 (t, ^3J = 7.2 Hz, 2H), 2.45 (s, 3H), 1.85 (m, 2H), 1.70 (m, 2H).

4,4'-bis(4-Bromo-1-butyl)-2,2'-bipyridine (bpy(C$_4$Br)$_2$)

This ligand was synthesized as described elsewhere [61].

Overall yield: 4% (M = 424.01 g mol^{-1}, $C_{18}H_{22}N_2Br_2$), ^{1}H-NMR (300 MHz; $CDCl_3$): ∂ (ppm) = 8.56 (d, 2H), 8.25 (d, 2H), 7.15 (s, 2H), 3.44 (m, 4H), 2.75 (t, 4H), 1.95-1.80 (m, 8H).

7-(7-Bromo-1-heptyl)-4'-(Methyl)-2,2'-bipyridine (bpyC$_7$Br)

In a 100 mL Schlenk flask, distilled diisopropylamine (1.9 mL, 16.4 mmol) was added to dry THF (30 mL) under nitrogen. The solution was cooled to -68 °C and *n*-butyllithium (5.26 mL, 13.1 mmol) was added dropwise. The resulting solution was stirred at this temperature over a period of one hour. The solution was allowed to come to room temperature.

In a 250 mL round bottom flask, 4,4'-dimethyl-2,2'-bipyridine (2.02 g, 11.0 mmol) was solubilized in dry THF (100 mL) and cooled to -68 °C. Then, the above-prepared solution of LDA was added dropwise over a period of 30 min after which the solution was stirred for another 45 min. Finally, the resulting solution was allowed to return to room temperature.

In a flask of 500 mL, the above-prepared bipyridine solution was added to a cooled solution (-68°C) of 1,6-dibromohexane (53 g, 220 mmol) in dry THF. The resulting solution was stirred for one hour and allowed to return to room temperature. Finally, the solution was stirred at room temperature for 14 hours.

The reaction was quenched with 10 mL of acidic water (1 mL HBr 48%) and the solution was concentrated under vacuum. Then, 40 mL of HBr 25 % was added after which the aqueous phase was extracted with chloroform. After evapo-

ration of the chloroform, the remaining the oil was mixed with a small quantity of chloroform (or ether) and the precipitate was filtered off and washed with cold chloroform and ether.

The protonated bipyridine (2.1 g) was then solubilized in water and Na_2CO_3 was added until neutrality was reached. The water was extracted with chloroform and the organic phase was evaporated giving a pinkish oil. This oil was dried under vacuum over night at 50 °C giving a pinkish solid.

Yield : 34% (M = 347.30 g mol^{-1}, $C_{18}H_{23}N_2Br$), Mass Spectrometry (ESI-MS, m/z): 347.11, ^{1}H-NMR (300 MHz; CD_2Cl_2): ∂ (ppm) = 8.55 (m, 2H), 8.25 (s, 2H), 7.14 (d, ^{3}J = 7.1 Hz, 2H), 3.40 (t, ^{3}J = 6.9 Hz, 2H), 2.70 (t, ^{3}J = 7.2 Hz, 2H), 2.45 (s, 3H), 1.85 (m, 4H), 1.70 (m, 4H), 1.40-1.35 (m, 2H).

7,7'-bis(7-Bromo-1-heptyl)-2,2'-bipyridine (bpy(C_7Br)$_2$)

In a 100 mL Schlenk flask, distilled diisopropylamine (3.8 mL, 32.8 mmol) was added to dry THF (30 mL). The solution was cooled to -68°C. n-Butyllithium (10.52 mL, 26.2 mmol) was added dropwise. Then, the solution was stirred over a period of one hour and allowed to reach room temperature.

In a 250 mL flask, 4,4'-dimethyl-2,2'-bipyridine (2.00 g, 10.9 mmol) was solubilized in dry THF (100 mL) and cooled to -68°C. Then, the freshly prepared LDA solution was added dropwise over a period of 30 min after which the solution was stirred for another 45 min. After this period the solution was allowed to reach room temperature.

In a 500 mL flask, the above-prepared bipyridine solution was added to a cooled solution (-68°C) of 1,6-dibromohexane (53 g, 220 mmol) in dry THF. After stiring for one hour at -68° the solution was allowed to reach room temperature where it was stirred for another 14 hours. The reaction was quenched with 10mL of acidic water (1 mL HBr 48%) and the solution was concentrated under vacuum. After the removal of THF under vacuum, water (50 mL) was added and the aqueous phase was extracted with chloroform. The chloroform was evaporated and the resulting pinkish oil was purified by chromatography on silica using a dichloromethane/ethyl acetate (7:1) as eluent. Finally, the solid was dried at 40°C under vacuum for one night.

Yield: 52% (M= 510.36 g mol^{-1}, $C_{24}H_{34}N_2Br_2$), ^{1}H-NMR (300 MHz; CD_2Cl_2): ∂ (ppm) = 8.55 (m, 2H), 8.26 (s, 2H), 7.14 (d, ^{3}J = 7.1Hz, 2H), 3.41 (t, ^{3}J = 6.9Hz, 2H), 2.72 (t, ^{3}J = 7.5Hz, 2H), 1.85 (m, 2H), 1.71 (m, 2H), 1.42-1.34 (m, 6H)

General way to Prepare Ruthenium Complexes

A solution of [Ru(bpy)$_2$Cl$_2$] (1 equivalent) and bromoalkylbipyridine (1.05 equivalent) in DMF was degassed and then heated at 90 °C for 100 hours under nitrogen.

After this period, the DMF was removed under vacuum *via* azeotropic distillation with toluene. The remaining solid was solubilized in water and washed multiple times with chloroform. The water layer was then concentrated and the compound was precipitated with ammonium hexafluorophosphate. The compound was purified by column chromatography on silica gel using acetonitrile/water/methanol/ sodium chloride 4:1:1:0.1 as eluent. After removal of the organic solvents, the product was precipitated from the remaining water phase by adding ammonium hexafluorophosphate. The precipitate was filtered off over celite, washed with water and dried with ether. The product was re-extracted from celite by addition of acetonitrile.

The product was dried at 50 °C under vacuum over night.

bpy$_2$RubpyC$_4$Br

Yield : 28% (M = 1008.59 g mol^{-1}, $C_{35}H_{33}N_6BrRuP_2F_{12}$), ^{1}H-NMR (300 MHz; CD_3CN): ∂ (ppm) = 8.52-8.49 (d, ^{3}J = 8.4 Hz, 4H), 8.41 (s, 1H), 8.39 (s, 1H), 8.10-8.03 (m, 4H), 7.75-7.73 (d, ^{3}J = 5.4 Hz, 4H), 7.61-7.54 (m, 2H), 7.44-7.36 (m, 4H), 7.27-7.24 (m, 2H), 3.66-3.62 (m, 2H), 2.87-2.74 (t, ^{3}J = 5.1 Hz, 2H), 2.57 (s, 3H), 1.85 (m, 4H).

bpy$_2$Rubpy(C$_4$Br)$_2$

Yield: 31% (M = 1129.57 g mol^{-1}, $C_{38}H_{38}N_6Br_2RuP_2F_{12}$), ^{1}H-NMR (300 MHz; CD_3CN): ∂ (ppm) = 8.52-8.49 (d, ^{3}J = 8.4 Hz, 4H), 8.41 (s, 1H), 8.39 (s, 1H), 8.10-8.03 (m, 4H), 7.75-7.73 (d, ^{3}J = 5.1 Hz, 4H), 7.61-7.54 (m, 2H), 7.44-7.36 (m, 4H), 7.27-7.24 (m, 2H), 3.66-3.62 (m, 4H), 2.87-2.74 (m, 4H), 1.85 (m, 8H).

bpy$_2$RubpyC$_7$Br

Yield: 37% (M = 1050.67 g mol^{-1}, $C_{38}H_{39}N_6BrRuP_2F_{12}$), ^{1}H-NMR (300 MHz; CD_3CN): ∂ (ppm) = 8.52-8.49 (d, ^{3}J = 8.4 Hz, 4H), 8.40 (s, 1H), 8.35 (s, 1H), 8.10-8.03 (t, ^{3}J = 5.1Hz, 4H), 7.75-7.73 (d, ^{3}J = 5.1 Hz, 4H), 7.61-7.54 (dd, ^{3}J = 5.7 Hz, 2H), 7.44-7.36 (dd, ^{3}J = 6.3 Hz, ^{4}J = 1.5 Hz, 4H), 7.25-7.23 (d, ^{3}J = 6.3 Hz, 2H), 3.62-3.59 (t, ^{3}J = 7.2 Hz, 2H), 2.83-2.78 (t, ^{3}J = 6.9 Hz, 2H), 2.55 (s, 3H), 1.72 (m, 2H), 1.54 (m, 2H), 1.39 (m, 6H).

bpy$_2$Rubpy(C$_7$Br)$_2$

Yield: 22% (M = 1213.73 g mol^{-1}, $C_{44}H_{50}N_6Br_2RuP_2F_{12}$), ^{1}H-NMR (300 MHz; CD_3CN): ∂ (ppm) = 8.51-8.48 (d, ^{3}J = 8.4 Hz, 4H), 8.40 (s, 1H), 8.36 (s, 1H), 8.12-8.02 (t, ^{3}J = 5.1 Hz, 4H), 7.76-7.73 (d, ^{3}J = 5.1 Hz, 4H), 7.61-7.54 (d, ^{3}J = 5.7 Hz, 2H), 7.44-7.36 (d, ^{3}J = 6.6 Hz, 4H), 7.25-7.23 (d, ^{3}J = 6.3 Hz, 2H), 3.62-3.59 (t, ^{3}J = 7.2 Hz, 4H), 2.83-2.77 (t, ^{3}J = 7.2 Hz, 4H), 1.70 (m, 4H), 1.55 (m, 4H), 1.39 (m, 12H).

General Procedure to Prepare Thioacetate Ruthenium Complexes

The bromoalkyl ruthenium complex (about 80 mg) and Amberlyte (bearing thioacetic acid as functional groups) (500 mg) in acetone (30mL) were stirred at room temperature for 4 days. After this period, the Amberlyte was filtered off and the acetone was evaporated. This operation was repeated 4 times with Amberlyte® and acetone being freshly added after each step. After the fourth cycle, the solid was dissolved into acetonitrile/water/methanol/sodium chloride 4:1:1:0.1. The acetonitrile and the methanol were evaporated. Finally, ammonium hexafluorophosphate was added to precipitate the ruthenium complex from the remaining water phase. The orange solid was filtered off over celite, washed with water, dried with ether and re-extracted with acetonitrile. After evaporation of acetonitrile, the resulting product was dried under vacuum over night.

bpy$_2$RubpyC$_4$S(CO)Me

Yield: 60% (M = 1003.80 g mol^{-1}, $C_{37}H_{36}N_6SORuP_2F_{12}$), Mass spectrometry (ESI, m/z) : 858.77 (M - PF_6) (M - PF_6),

356.86 (M – 2 PF_6), (M - PF_6), 358.37 (M – 2 PF_6), (HR-MS): 358.9282 (M – 2 PF_6), ^{1}H-NMR (300 MHz; CD_3CN): ∂ (ppm) = 8.52-8.49 (d, ^{3}J = 8.4 Hz, 4H), 8.40 (s, 1H), 8.37 (s, 1H), 8.10-8.03 (t, ^{3}J = 7.8 Hz, 4H), 7.75-7.73 (d, ^{3}J = 4.8 Hz, 4H), 7.61-7.54 (dd, ^{3}J = 5.7 Hz, 2H), 7.44-7.36 (dd, ^{3}J = 6.3 Hz, ^{4}J = 1.5 Hz, 4H), 7.25-7.23 (d, ^{3}J = 6.3Hz, 2H), 2.86-2.78 (t, ^{3}J = 6.9 Hz, 4H), 2.55 (s, 3H), 2.28 (s, 3H), 1.80 (m, 2H), 1.56 (m, 2H), 1.39 (m, 6H).

bpy$_2$Rubpy(C$_4$S(CO)Me)$_2$

Yield: 82% (M = 1119.97 g mol^{-1}, $C_{42}H_{44}N_6S_2O_2RuP_2F_{12}$), Mass spectrometry (ESI-MS, m/z): 975.16 (M - PF_6), 415.11 (M – 2 PF_6), (HR-MS): 415.10026 (M – 2 PF_6), ^{1}H-NMR (300 MHz; CD_3CN): ∂ (ppm) = 8.52-8.50 (d, ^{3}J = 8.4 Hz, 4H), 8.40 (s, 1H), 8.38 (s, 1H), 8.10-8.03 (m, 4H), 7.75-7.73 (d, ^{3}J = 5.7 Hz, 4H), 7.61-7.54 (d, ^{3}J = 5.7 Hz, 2H), 7.46-7.36 (m, 4H), 7.26-7.23 (m, 2H), 2.93-2.81 (m, 8H), 2.31 (s, 6H), 1.72 (m, 4H), 1.64 (m, 4H).

bpy$_2$RubpyC$_7$S(CO)Me

Yield: 86% (M = 1045.88 g mol^{-1}, $C_{40}H_{42}N_6SORuP_2F_{12}$), Mass spectrometry (ESI-MS, m/z) : 901.18 (M - PF_6), 378.11 (M – 2 PF_6), (HR-MS): 378.10953 (M – 2 PF_6), ^{1}H-NMR (300 MHz; CD_3CN) : ∂ (ppm) = 8.52-8.49 (d, ^{3}J = 8.4 Hz, 4H), 8.40 (s, 1H), 8.35 (s, 1H), 8.10-8.03 (t, ^{3}J = 5.1 Hz, 4H), 7.75-7.73 (d, ^{3}J = 5.1 Hz, 4H), 7.61-7.54 (dd, ^{3}J = 5.7 Hz, 2H), 7.44-7.36 (dd, ^{3}J = 6.3 Hz, ^{4}J = 1.5 Hz, 4H), 7.25-7.23 (d, ^{3}J = 6.3 Hz, 2H), 2.86-2.78 (t, ^{3}J = 6.9 Hz, 4H), 2.55 (s, 3H), 2.28 (s, 3H), 1.72 (m, 2H), 1.54 (m, 4H), 1.39 (m, 6H).

bpy$_2$Rubpy(C$_7$S(CO)Me)$_2$

Yield: 55.6 % (M = 1204.13 g mol^{-1}, $C_{48}H_{56}N_6S_2O_2RuP_2F_{12}$), Mass spectrometry (ESI, m/z) : 1059.17 (M - PF_6), 457.14716 (M – 2 PF_6), (HR-MS): 415.10026 (M – 2 PF_6), ^{1}H-NMR (300 MHz; CD_3CN) : ∂ (ppm) = 8.53-8.48 (d, ^{3}J = 8.4 Hz, 4H), 8.39 (s, 1H), 8.35 (s, 1H), 8.10-8.03 (t, ^{3}J = 5.1 Hz, 4H), 7.75-7.73 (d, ^{3}J = 5.1 Hz, 4H), 7.60-7.54 (dd, ^{3}J = 5.7 Hz, 2H), 7.44-7.34 (d, ^{3}J = 6.6 Hz, 4H), 7.24-7.22 (d, ^{3}J = 6.6 Hz, 2H), 2.90-2.79 (m, 8H), 2.28 (s, 6H), 1.72 (m, 4H), 1.54 (m, 8H), 1.39 (m, 12H).

General Procedure for the Thiol de-Protection in the Ruthenium Complexes

In a 50 mL flask, the protected thiol-ruthenium complex was solubilized into DMF. The solution was degassed, hydrazine (1.5 Eq) was added and the reaction was stirred for 1 hour at room temperature. The solution was neutralized adding acetic acid. The solution of DMF was then poured into a solution of ammonium hexafluorophosphate in water. The orange solid was filtered off over celite, wash with water, dried with ether and re-extracted with acetonitrile. Note that the de-protection is done just immediately prior the measurements.

5. REFERENCES

[1] Flink, S.; van Veggel, F.; Reinhoudt, D. N. *J. Phys. Org. Chem.*, **2001,** *14*, 407.

[2] Tai, Y.; Shaporenko, A.; Rong, H. T.; Buck, M.; Eck, W.; Grunze, M.; Zharnikov, M. *J. Phys. Chem. B*, **2004,** *108*, 16806.

[3] Belser, T.; Stohr, M.; Pfaltz, A. *J. Am. Chem. Soc.,* **2005,** *127*, 8720.

[4] Sasahara, A.; Pang, C. L.; Onishi, H. *J. Phys. Chem. B,* **2006,** *110*, 4751.

[5] Yokoyama, T.; Yokoyama, S.; Kamikado, T.; Okuno, Y.; Mashiko, S. *Nature*, **2001,** *413*, 619.

[6] van Manen, H. J.; Auletta, T.; Dordi, B.; Schonherr, H.; Vancso, G. J.; van Veggel, F.; Reinhoudt, D. N. *Adv. Funct. Mater.*, **2002,** *12*, 811.

[7] Figgemeier, E. M. L.; Hermann, B. A.; Zimmermann, Y. C.; Housecroft, C. E.; Guentherodt, H. J.; Constable, E. C. *J. Phys. Chem. B*, **2003,** *107*, 1157.

[8] Figgemeier, E.; Constable, E. C.; Housecroft, C. E.; Zimmermann, Y. C. *Langmuir*, **2004,** *20*, 9242.

[9] Crespo-Biel, O.; Dordi, B.; Reinhoudt, D. N.; Huskens, J. *J. Am. Chem. Soc.*, **2005,** *127*, 7594.

[10] Scherer, L. J.; Merz, L.; Constable, E. C.; Housecroft, C. E.; Neuburger, M.; Hermann, B. A. *J. Am. Chem. Soc.*, **2005,** *127*, 4033.

[11] Hermann, B. A.; Scherer, L. J.; Housecroft, C. E.; Constable, E. C. *Adv. Funct. Mater.*, **2006,** *16*, 221.

[12] Weidner, T.; Kraemer, A.; Bruhn, C.; Zharnikov, M.; Shaporenko, A.; Siemeling, U.; Traeger, F. *Dalton Trans.*, **2006**, 2767.

[13] Fox, M. A. *Electron Transfer in Chemistry*, Balzani, Vincenzo. ed.; Wiley-VCH Verlag GmbH: Weinheim, Germany, **2001**.

[14] Lukas, A. S.; Wasielewski, M. R. *Electron Transfer in Chemistry*, Balzani, Vincenzo. ed.; Wiley-VCH Verlag GmbH.: Weinheim, Germany, **2001**.

[15] Gust, D.; Moore, T. A.; Moore, A. L. *Accounts Chem. Res.*, **1993,** *26*, 198.

[16] De Cola, L.; Belser, P. *Coord. Chem. Rev.*, **1998,** *177*, 301.

[17] Bakker, B. H.; Goes, M.; Hoebe, N.; van Ramesdonk, H. J.; Verhoeven, J. W.; Werts, M. H. V.; Hofstraat, J. W. *Coord. Chem. Rev.*, **2000,** *208*, 3.

[18] Bignozzi, C. A.; Argazzi, R.; Kleverlaan, C. J. *Chem. Soc. Rev.*, **2000,** *29*, 87.

[19] Gust, D.; Moore, T. A.; Moore, A. L. *Accounts Chem. Res.*, **2001,** *34*, 40.

[20] Li, C.; Fan, W.; Straus, D. A.; Lei, B.; Asano, S.; Zhang, D. H.; Han, J.; Meyyappan, M.; Zhou, C. W. *J. Am. Chem. Soc.*, **2004,** *126*, 7750.

[21] Li, C.; Fan, W. D.; Lei, B.; Zhang, D. H.; Han, S.; Tang, T.; Liu, X. L.; Liu, Z. Q.; Asano, S.; Meyyappan, M.; Han, J.; Zhou, C. W. *Appl. Phys. Lett.*, **2004,** *84*, 1949.

[22] Flink, S.; van Veggel, F.; Reinhoudt, D. N. *Adv. Mater.*, **2000,** *12*, 1315.

[23] Zimmerman, R.; Basabe-Desmonts, L.; van der Baan, F.; Reinhoudt, D. N.; Crego-Calama, M. *J. Mater. Chem.*, **2005,** *15*, 2772.

[24] Scandola, F.; Bignozzi, C. A.; Chiorboli, C.; Indelli, M. T.; Rampi, M. A. *Coord. Chem. Rev.*, **1990,** *97*, 299.

[25] Pullerits, T.; Sundstrom, V. *Accounts Chem. Res.*, **1996,** *29*, 381.

[26] Balzani, V.; Ceroni, P.; Maestri, M.; Saudan, C.; Vicinelli, V. In *Dendrimers V: Functional and Hyperbranched Building Blocks, Photophysical Properties, Applications in Materials and Life Sciences*; Springer-Verlag Berlin: Berlin, **2003**; pp. 159-191.

[27] Nierengarten, J. F.; Armaroli, N.; Accorsi, G.; Rio, Y.; Eckert, J. F. *Chem. Eur. J.*, **2003,** *9*, 37.

[28] Juris, A.; Balzani, V.; Barigelletti, F.; Campagna, S.; Belser, P.; Vonzelewsky, A. *Coord. Chem. Rev.*, **1988,** *84*, 85.

[29] Balzani, V.; Juris, A.; Venturi, M.; Campagna, S.; Serroni, S. *Chem. Rev.*, **1996,** *96*, 759.

[30] (a) Obeng, Y. S.; Bard, A. J. *Langmuir*, **1991,** *7*, 195. (b) Faiz, J.; Philippopoulos, A. I.; Kontos, A. G.; Falaras, P.; Pikramenou, Z. *Adv. Func. Mat.*, **2007**, *17*, 54.

[31] Sato, Y.; Uosaki, K. *J. Electroanal. Chem.*, **1995,** *384*, 57.

[32] Yamada, S.; Koide, Y.; Matsuo, T. *J. Electroanal. Chem.,* **1997,** *426*, 23.

[33] Panetta, C. A.; Kumpaty, H. J.; Heimer, N. E.; Leavy, M. C.; Hussey, C. L. *J. Org. Chem.*, **1999,** *64*, 1015.

[34] Kim, Y. T.; McCarley, R. L.; Bard, A. J. *J. Phys. Chem.*, **1992,** *96*, 7416.

[35] Smalley, J. F.; Finklea, H. O.; Chidsey, C. E. D.; Linford, M. R.; Creager, S. E.; Ferraris, J. P.; Chalfant, K.; Zawodzinsk, T.; Feldberg, S. W.; Newton, M. D. *J. Am. Chem. Soc.*, **2003,** *125*, 2004.

[36] Smalley, J. F.; Newton, M. D.; Feldberg, S. W. *J. Electroanal. Chem.*, **2006,** *589*, 1.

[37] (a) Bertoncello, P.; Kefalas, E. T.; Pikramenou, Z.; Unwin, P. R.; Forster, R. J. *J. Phys. Chem. B*, **2006,** *110*, 10063. (b) Silva, M. J. J.

P.; Bertoncello, P.; Daskalakis, N. N.; Spencer, N.; Kariuki, B. M.; Unwin, P.R.; Pikramenou, Z. *Supramol. Chem.*, **2007,** *19*, 115.
[38] Kittredge, K. W.; Fox, M. A.; Whitesell, J. K. *J. Phys. Chem. B*, **2001,** *105*, 10594.
[39] Shepherd, J. L.; Kell, A.; Chung, E.; Sinclar, C. W.; Workentin, M. S.; Bizzotto, D. *J. Am. Chem. Soc.*, **2004,** *126*, 8329.
[40] Geddes, C. D.; Parfenov, A.; Roll, D.; Gryezynski, I.; Malicka, J.; Lakowicz, J. R. *Spectroc. Acta Pt. A-Molec. Biomolec. Spectr.*, **2004,** *60*, 1977.
[41] Zhang, J.; Lakowicz, J. R. *J. Phys. Chem. B*, **2005,** *109*, 8701.
[42] Zhang, J.; Malicka, J.; Gryczynski, I.; Lakowicz, J. R. *J. Phys. Chem. B*, **2005,** *109*, 7643.
[43] Wang, T. X.; Zhang, D. Q.; Xu, W.; Yang, J. L.; Han, R.; Zhu, D. B. *Langmuir*, **2002,** *18*, 1840.
[44] Lee, I. Y. S.; Suzuki, H.; Ito, K.; Yasuda, Y. *J. Phys. Chem. B*, **2004,** *108*, 19368.
[45] Fleischmann, M.; Hendra, P. J.; McQuillan, A. J. *Chem. Phys. Lett.*, **1974,** *26*, 163.
[46] Albrecht, M. G.; Creighton, J. A. *J. Am. Chem. Soc.*, **1977,** *99*, 5215.
[47] Jeanmaire, D. L.; Van Duyne, R. P. *J. Elect. Chem. Interfacial. Electrochem.*, **1977,** *84*, 1.
[48] Hartstein, A.; Kirtly, J. R.; Tsang, C. T. *Phys. Rev. Lett.*, **1980,** *45*, 201.
[49] Nakao, Y.; Yamada, H. *Appl. Phys.*, **1986,** *176*, 578.
[50] Kamata, T.; Kato, A.; Umemura, J.; Takenaka, T. *Langmuir*, **1987**, 1150.
[51] Osawa, M.; Ataka, K.; Ikeda, M.; Uchihara, H. *Anal. Sci.*, **1991**, 503.
[52] Cainelli, G.; Contento, M.; Manescalchi, F.; Mussatto, M. C. *Synthesis*, **1981,** *4*, 302.
[53] Nicolaides, E. D.; Tinney, F. J.; Kaltenbronn, J. S.; Repine, J. T.; DeJohn, D. A.; Lunney, E. A.; Roark, W. H. *J. Med. Chem.*, **1986,** *29*, 959.
[54] Valenty, S. J.; Behnken, D. E.; Gaines, G. L. Jr. *Inorg. Chem.*, **1979,** *18*, 2160.
[55] Johansen, O.; Kowala, C.; Mau, A. W. H.; Sasse, W. H. F. *Aust. J. Chem.*, **1979,** *32*, 2395.
[56] Other attempts using a mixture of butanethiol (10 equivalent) and **bpy$_2$RubpyC$_7$SH** or **bpy$_2$Rubpy(C$_7$SH)$_2$** (1 equivalent) or using an already prepared monolayer (with butanethiol) then substituting with **bpy$_2$RubpyC$_7$SH** or **bpy$_2$Rubpy(C$_7$SH)$_2$** give the same result.
[57] Contact angle values were 70° ± 2° for the pristine gold surface and 50° ± 4° for self assembled layers of all the complexes on gold.
[58] Bohmer, M.; Enderlein, J. *J. Opt. Soc. Am. B-Opt. Phys.*, **2003,** *20*, 554.
[59] Piwonski, H.; Stupperich, C.; Hartschuh, A.; Sepiol, J.; Meixner, A.; Waluk, J. *J. Am. Chem. Soc.*, **2005,** *127*, 5302.
[60] Lakowicz, J. R. *Principles of Fluorescence Spectroscopy*, 2nd ed. ed.; Kluwer Academic/Plenum Publisher: New York, **1999**.
[61] Chambron, J.-C.; Sauvage, J.-P. *Tetrahedron*, **1987,** *43*, 895.

Received: July 12, 2007 Revised: July 19, 2007 Accepted: July 19, 2007